Effects of Ag^I, Au^III, and Cu^II on the Reductive Dechlorination of Carbon Tetrachloride by Green Rust

EDWARD J. O'LOUGHLIN,*,†,‡
KENNETH M. KEMNER,‡ AND
DAVID R. BURRIS†,§

Air Force Research Laboratory, AFRL/MLQL, 139 Barnes Drive, Tyndall Air Force Base, Florida, 32403-5323, Environmental Research Division, Argonne National Laboratory, 9700 South Cass Avenue, Argonne, Illinois 60439-4843, and Integrated Science and Technology, Inc., 433 Harrison Avenue, Panama City, Florida 32401

Green rusts (GRs), mixed iron(II)/iron(III) hydroxide minerals found in many suboxic environments, have been shown to reduce a range of organic and inorganic contaminants, including several chlorinated hydrocarbons. Many studies have demonstrated the catalytic activity of transition metal species in the reduction of chlorinated hydrocarbons, suggesting the potential for enhanced reduction by GR in the presence of an appropriate transition metal catalyst. Reductive dechlorination of carbon tetrachloride (CT) was examined in aqueous suspensions of GR amended with Ag^I, Au^III, or Cu^II. The CT reduction rates were greatly increased for systems amended with Cu^II, Au^III, and Ag^I (listed in order of increasing rates) relative to GR alone. Observed intermediates and products included chloroform, dichloromethane, chloromethane, methane, acetylene, ethene, ethane, carbon monoxide, tetrachloroethene, and various nonchlorinated C_3 and C_4 compounds. Product distributions for the reductive dechlorination of CT were highly dependent on the transition metal used. A reaction pathway scheme is proposed in which CT is reduced primarily to methane and other nonchlorinated end products, largely through a series of one-electron reductions forming radicals and carbenes/carbenoids. Recently, X-ray absorption fine structure analysis of aqueous GR suspensions amended with Ag^I, Au^III, or Cu^II showed that the metals were reduced to their zerovalent forms. A possible mechanism for CT reduction is the formation of a galvanic couple involving the zerovalent metal and GR, with reduction of CT occurring on the surface of the metal and GR serving as the bulk electron source. The enhanced reduction of CT by GR suspensions amended with Ag^I, Au^III, or Cu^II may prove useful in the development of improved materials for remediation of chlorinated organic contaminants.

Introduction

Green rusts (GRs) are mixed ferrous/ferric hydroxides that have structures consisting of alternating positively charged hydroxide layers and hydrated anion layers with the general composition

$$[Fe^{II}_{(6-x)}Fe^{III}_x(OH)_{12}]^{x+}[(A)_{x/n}yH_2O]^{x-} \quad (1)$$
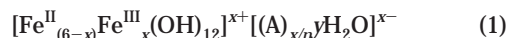
where $x = 0.9−4.2$, A is an n-valent anion (typically Cl^-, SO_4^{2-}, or CO_3^{2-}, although GRs containing Br^-, I^-, NO_3^-, ClO_4^-, SO_3^{2-}, SeO_4^{2-}, and oxalate have been prepared), and y denotes the varying amounts of interlayer water (typically $y = 2−4$ for most GRs). Green rusts typically form under neutral to alkaline conditions in suboxic environments, and they have been identified as products of both abiotic and microbially induced corrosion of iron and steel (*1−4*), the microbially mediated (*5*, *6*) and abiotic (*7*, *8*) reductive dissolution of ferric oxyhydroxides by Fe^{2+}, and the biooxidation of Fe^{2+} (*9*). Green rusts are readily synthesized in the laboratory via the oxidation of ferrous hydroxide by molecular oxygen at circumneutral pH (*10*, *11*). Oxidation of GRs results in the formation of ferrihydrite, goethite (α-FeOOH), akaganeite (β-FeOOH), lepidocrocite (γ-FeOOH), δ-FeOOH, maghemite (γ-Fe_2O_3), or magnetite (Fe_3O_4) depending upon pH, solution composition, oxidant, rate of oxidation, and degree and rate of dehydration (*12−17*).

The characteristic bluish-green color of hydromorphic soils has long been presumed to be due to the presence of mixed iron(II)/iron(III) hydroxide species (*18*); however, the unambiguous identification of GRs in suboxic soils and sediments has been complicated by the rapid oxidation of these compounds upon exposure to air. Direct evidence for the presence of GRs in hydromorphic soils has recently been reported (*19*, *20*), and the material has been tentatively identified as hydroxy-GR (GR_OH) (*21*). Recent work by Bourrié et al. (*22*) suggests that the solubility of Fe in soil solutions of hydromorphic soils is controlled by equilibrium with GR_OH. As metastable intermediates in the transformation of Fe^II to magnetite and iron(III) oxyhydroxides (e.g., lepidocrocite and goethite) at near-neutral to slightly alkaline pH, GRs are believed to play a central role in the redox cycling of Fe in aquatic and terrestrial environments. In addition, recent research suggests that GRs may be highly reactive reductants in suboxic environments. Green rusts are capable of reducing a number of organic and inorganic contaminants, including uranyl (*23*), nitrate and nitrite (*24*, *25*), selenate (*26*), chromate (*27*, *28*), and halogenated hydrocarbons (*29−31*); these observations suggest that GRs may play an important role in the fate and transport of contaminants in suboxic soils and sediments.

The reductive transformation of many organic and inorganic contaminants is thermodynamically favored in suboxic environments and often results in the formation of products considered to be less hazardous than the parent compound; however, these reactions are often kinetically constrained. The rate of reductive dehalogenation of chlorinated hydrocarbons by GR is typically slower than the rate for Fe^0 (*30*, *32*), the most commonly used material for the construction of permeable reactive barriers (PRBs) (*33*). However, studies demonstrating the catalytic activity of transition metal species in the reduction of a range of contaminants by a number of bulk reductants (*34−43*) suggest the potential for enhanced contaminant reduction by GR in the presence of certain metals. This paper examines the effects of Ag^I, Au^III, and Cu^II on the rate and product distribution for the reductive dechlorination of carbon tetrachloride in aqueous suspensions of GR.

* Corresponding author e-mail: oloughlin@anl.gov; telephone: (630)252-9902; fax: (630)252-5498.
† Air Force Research Laboratory.
‡ Argonne National Laboratory.
§ Integrated Science and Technology, Inc.

Experimental Section

Chemicals and Reagents. Chloromethane (CM, 99.5%); tetrachloroethene (perchloroethene (PCE), 99.5%); iron(II) sulfate heptahydrate (99+%); silver(I) acetate (99.999%); copper(II) chloride (99.999%); propene (99+%); 1-butene (99+%); n-heptane (99+%); a mixture of cis- and $trans$-2-butene (38.1% cis and 61.6% trans); and nanoparticulate activated powders of Ag^0, Au^0, and Cu^0 (99.9+%) were obtained from Aldrich. Tetrachloromethane (carbon tetrachloride (CT), 100%) and dichloromethane ((DCM), 99.5%) were purchased from Chem Service. Trichloromethane (chloroform (CF), HPLC grade) was purchased from Fisher. Propane (1.002% in N_2), n-butane (1.0% in N_2), carbon monoxide (10.0% in He), and a multicomponent gas mixture containing methane, ethane, ethene, and acetylene (each at 1.0 mol % in N_2) were purchased from Scott Specialty Gases. Gold(III) chloride was purchased from Sigma. Chemicals were of reagent grade unless otherwise indicated.

Hydroxysulfate GR (GR_{SO_4}), a GR in which the interlayer anion is SO_4^{2-}, was synthesized by air oxidation of a 1.0 M ferrous sulfate solution. Briefly, 278 g of $FeSO_4 \cdot 7H_2O$ was dissolved in 1 L of distilled deionized water on a magnetic stirrer under ambient atmosphere. Upon dissolution, 1.0 M NaOH was added dropwise until the pH remained stable at 7.0, at which point the GR_{SO_4} suspension was placed in a glovebox. All subsequent handling occurred in an anoxic atmosphere (4−6% H_2 in N_2). The GR was recovered by centrifugation and subsequently washed four times with distilled deionized water. The specific surface area of a freeze-dried subsample of the GR_{SO_4} suspension was measured by five-point Brunauer−Emmett−Teller (BET) gas adsorption with N_2. Exposure to air during the BET measurement was minimized by using a Quantachrome cell-seal assembly. Magnetite was prepared as described by Cornell and Schwertmann (*44*).

Experimental Setup. The reaction system consisted of 160-mL serum vials crimp-sealed with Teflon-lined rubber septa. Each vial contained 94 mL of distilled deionized water, 5 mL of GR_{SO_4} suspension ($\sim$0.5 g of GR_{SO_4}), 1 mL of either 0.1 M HCl or 10^{-2} M Au^{III} or Cu^{II} in 0.1 M HCl, and 0.1 mL of 1.0 M NaOH. Systems containing Ag^I were prepared as described above; however, the Ag^I stock solution was prepared in distilled deionized water, and NaOH was not added. All preparative work was performed in an anoxic glovebox. The vials were sealed and spiked with 5 μmol of n-heptane (5 μL of a 1.0 M methanolic solution of n-heptane) that served as an internal standard. Reduction reactions were initiated by spiking with 2 μmol of a given chlorinated methane (2 μL of 1.0 M methanolic solutions of either CT, CF, or DCM or 50 μL of CM gas at standard temperature and pressure). Initial solution concentrations were 0.5 g of GR_{SO_4} in 100 mL and 100 μM for Ag^I, Au^{III}, and Cu^{II}; the total mass of chlorinated methane added to each vial was 2 μmol. The vials were placed on a roller drum (rotating vertically as the bottle axis remained horizontal) in an incubator maintained at 20 °C. For reactions with fast kinetics (reaction complete in <15 min), the vials were vigorously shaken by hand under ambient conditions. The initial pH of the experimental systems was 7.6 ± 0.1. During the reductive dehalogenation experiments the pH was allowed to change freely; however, the pH was measured at the end of each experiment and in all cases was within 0.5 pH units of the initial value. Reduction of CT by magnetite and by zerovalent Ag, Au, or Cu was examined as described for GR but with 0.5 g of hydrated magnetite or 0.1 g of Ag^0, Au^0, or Cu^0 in place of the GR.

Analytical Methods. At selected intervals, 200-μL headspace samples were removed from the serum vials for analysis with a Hewlett-Packard 5890 series II gas chromatograph (GC) with a GSQ column (0.53 mm i.d. by 30 m) and a flame

ionization detector (FID; 240 °C). Samples were injected in split mode (split ratio 2:1) with the injector at 180 °C. Helium was used as the carrier gas. The oven temperature was held at 50 °C for 2 min, ramped at 25 °C min^{-1}, and held at 200 °C for 10 min. The system was calibrated by equilibrating known masses of analytes and internal standard (n-heptane) in serum vials containing the same ratio of aqueous phase to vapor phase as the experimental systems, thus accounting for water−vapor partitioning and allowing analyte concentration to be expressed as mass per bottle. Vapor−liquid partitioning in these systems was rapid relative to the reaction kinetics. For reactions with fast kinetics, CT and CF were analyzed on an identical GC equipped with a 0.53 mm i.d,, 30 m long DB-1 column under isothermal conditions at 50 °C. Samples were injected in split mode (split ratio 2:1) at 200 °C with helium as the carrier gas. The FID temperature in this second GC was 200 °C.

Analysis of carbon monoxide in headspace samples was performed by using a Trace Analytical (Menlo Park, CA) RGA3 reduction gas analyzer with an oven temperature of 266 °C. Formate was analyzed by using a Dionex LC20 ion chromatograph with self-regenerating suppressor control. An IONPAC AG11 guard column (4 × 50 mm) and an IONPAC AG11 analytical column (4 × 250 mm) were used with a weakly basic eluent (NaOH, 350 μmol L^{-1}) at a flow rate of 1.0 mL min^{-1}.

X-ray diffraction (XRD) analysis of GR_{SO_4} and its oxidation product(s) was performed using a Rigaku MiniFlex X-ray diffractometer with Ni-filtered Cu Kα radiation. Samples for XRD analysis were collected by centrifugation, and the resulting wet pastes were mixed with glycerol to minimize oxidation (*45*) and prepared as smears on 22 mm wide glass plates. The samples were scanned between 6° and 80° 2θ at a speed of 1° 2θ min^{-1}.

Kinetic Analysis. Apparent pseudo-first-order rate constants (k_{obs}) were obtained by fitting the data for mass of CT in the system over time to the exponential decay expression:

$$M_{CT_t} = M_{CT_0} e^{-k_{obs}t} \qquad (2)$$

where t refers to time, and M_{CT_t} and M_{CT_0} refer to the mass of CT in the system at times t and zero, respectively. For a reaction taking place only in the solution phase, the apparent pseudo-first-order rate constant that pertains to the reaction of a volatile constituent capable of rapid partitioning between the solution phase and the headspace (k_{obs}) is equivalent to the rate constant that would be obtained in a headspace-free system (k'_{obs}), as described by Burris et al. (*46*). Values of k'_{obs} were calculated using the "dimensionless" Henry's law constant for CT from Gossett (*47*).

Results and Discussion

Reduction of Carbon Tetrachloride. CT was reduced by GR, with approximately 33% of the initial mass remaining after 195 h (Figure 1). Overall, the reduction of CT by GR was not well described by first-order kinetics; however, CT reduction within the first 6 h was consistent with first-order kinetics (Figure 1) with a rate constant of 1.7×10^{-5} s^{-1}. The surface area of the GR_{SO_4} was 14.1 m^2 g^{-1}, resulting in a surface-area-normalized rate constant of 2.4×10^{-7} L s^{-1} m^{-2}. Although the experimental systems were quite different (prohibiting direct comparison), the observed first-order rate constant for the initial reduction of CT by GR in our system (1.7×10^{-5} s^{-1}) is within the range of rate constants for CT reduction by GR (0.47×10^{-5}−2.18×10^{-5} s^{-1}) reported by Erbs et al. (*29*).

The initial product in the reductive dechlorination of CT by GR was CF (Figure 1). After 575 h (24 d) and with 17% of the initial CT remaining, CF was the major product (Table
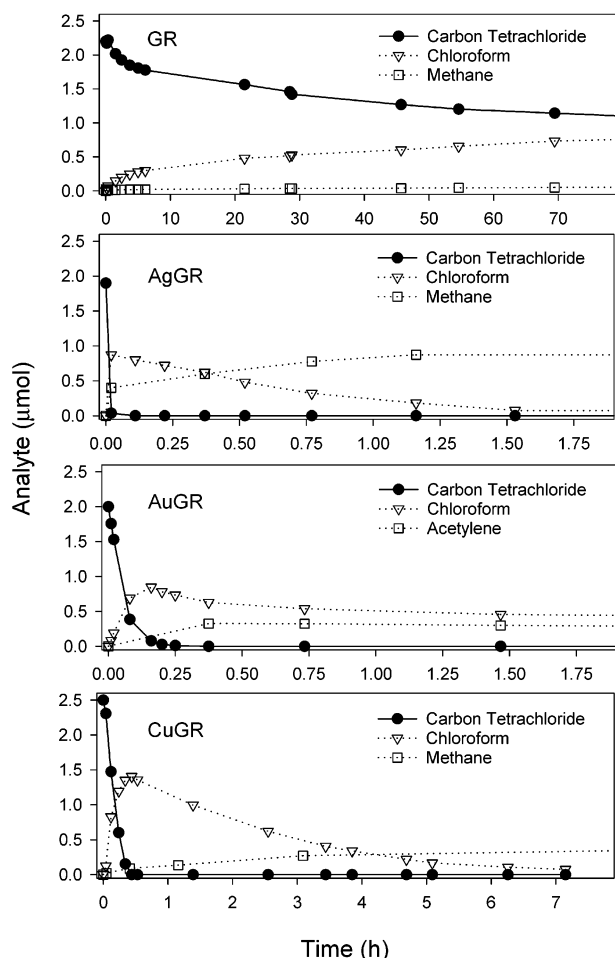
FIGURE 1. Degradation of CT by GR, AgGR, AuGR, and CuGR with appearance of major intermediates/products. Experiments were initiated by spiking 2 μmol of CT into 160-mL serum vials containing 100 mL of GR_{SO_4} suspension (0.5 g of GR_{SO_4}) with 100 μmol of Ag^I, Au^{III}, or Cu^{II} added as indicated.

TABLE 1. Final Product Distributions for CT Reduction by GR, AgGR, AuGR, and CuGR[a]

| | % of CT-derived C[b] | | | |
compound	GR	AgGR	AuGR	CuGR
carbon monoxide	29	4	trace	22
methane	4	33	11	26
chloromethane	nd	3	nd	1
dichloromethane	nd	7	4	7
chloroform	45	nd	8	nd
carbon tetrachloride	17	nd	nd	nd
total C_1 products	95	47	24	56
ethane	nd	1	1	1
ethene	nd	8	23	4
acetylene	nd	10	11	nd
tetrachloroethene	2	1	nd	1
total C_2 products	2	20	35	6
total C_3 products	nd	1	3	5
total C_4 products	nd	4	7	6
total recovered C	97	72	69	73

[a] Data are from final measurements made at 70 h (AuGR) or 575 h (GR, AgGR, and CuGR) after the experiments were initiated by spiking with 2 μmol of CT. [b] nd indicates not detected; trace indicates detected at <1%.

1) with minor amounts of methane and PCE; DCM and CM were not detected. Our results are in general agreement with the products reported by Erbs et al. (29) for the reductive

dechlorination of CT by GR. However, methane and CO accounted for 4% and 29% (respectively) of the mass of CT-derived C in our experiments, but they were not reported as products of CT reduction by GR by Erbs and co-workers (29). Additionally, Erbs et al. (29) reported the production of hexachloroethane (HCA) and PCE, but HCA was not detected in our experiments. However, O'Loughlin and Burris (31) reported that HCA is rapidly reduced to PCE by GR; thus, in our system HCA may have been an intermediate that was reduced to PCE before reaching detectable levels. The differences in the minor products observed in our experiments versus those reported by Erbs et al. (29) are likely due to differences in experimental conditions. Erbs and co-workers (29) examined CT reduction in GR suspensions containing aqueous CT concentrations at or near saturation due to the presence of bulk-phase CT. The relatively high aqueous solubility of CT and the presence of bulk-phase CT make competition for reactive sites between CT and HCA likely. Such competition may have been significant enough to slow the kinetics of HCA reduction sufficiently for it to accumulate to detectable levels. Given the substantially lower levels of CT (in terms of both total CT and the ratio of CT to GR) in our experiments, competition would likely be negligible, and thus HCA would be reduced rapidly to PCE.

As with GR alone, CT was reduced to CF with the addition of Ag^I, Au^{III}, or Cu^{II} although at dramatically enhanced rates (Figure 1). CT was reduced by GR to nondetectable levels in less than 12, 15, and 25 min in the systems amended with Ag^I, Au^{III}, and Cu^{II} (hereafter designated AgGR, AuGR, and CuGR), respectively. The disappearance of CT in AgGR, AuGR, and CuGR systems was well described by pseudo-first-order kinetics (with observed first-order rate constants of 8.7×10^{-2}, 8.3×10^{-3}, and 2.7×10^{-3} s^{-1}, respectively). Although there was little subsequent transformation of CF by GR alone, CF was completely transformed by AgGR and CuGR, and only 8% remained with AuGR. The terminal products of CT transformation observed with AgGR, AuGR, or CuGR were primarily nonchlorinated hydrocarbons (principally methane with lesser amounts of ethane, ethene, acetylene, and a suite of C_3 and C_4 alkanes and alkenes) and carbon monoxide with minor amounts of DCM, CM, and PCE (Table 1). The final carbon recovery (the fraction of CT-derived C accounted for by identified products) in AgGR, AuGR, and CuGR systems was less than 75%. In experimental controls without GR, Ag^I, Au^{III}, or Cu^{II} (i.e., water only), the loss of volatile compounds from the vials was less than 5% over the time scale of these experiments with no indication of biotic or abiotic transformation of CT, CF, DCM, or CM. Moreover, sorption of CT reduction products by GR was not significant; therefore, the incomplete recovery of C suggests the formation of unidentified products.

Reduction of Less Chlorinated Methanes. Chloroform was not readily reduced by GR alone. After a slight initial reduction, CF levels remained relatively constant (Figure 2) with 83% remaining after 1,152 h (48 d) (Table 2). Chloroform was completely transformed by AgGR and CuGR (and partially reduced by AuGR), although at substantially slower rates than for CT reduction. The distribution of products from the reduction of CF was similar to that observed for CT with methane being the primary product along with lesser amounts of DCM, CM, CO, and C_2–C_4 alkanes, alkenes, and alkynes.

Within the duration of the experiments (7 d for AuGR and 48 d for GR), DCM and CM were not transformed by GR or AuGR (Table S1, Supporting Information). Minor amounts (<10% after 48 d) of DCM were reduced by AgGR to CM and methane and by CuGR to methane. With AgGR and CuGR, CM was essentially nonreactive; however, trace levels of methane (<1%) were observed after 48 d.
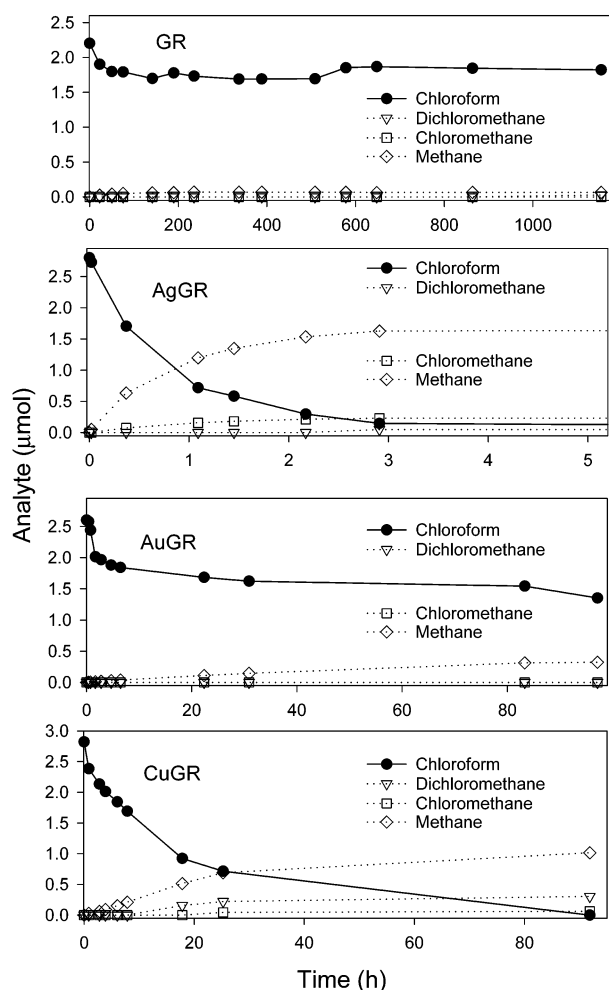
FIGURE 2. Degradation of CF by GR, AgGR, AuGR, and CuGR and appearance of major intermediates/products. Experiments were initiated by spiking 2 μmol of CF into 160-mL serum vials containing 100 mL of GR_{SO_4} suspension (0.5 g of GR_{SO_4}) with 100 μmol of Ag^I, Au^{III}, or Cu^{II} added as indicated.

TABLE 2. Final Product Distributions for CF Reduction by GR, AgGR, AuGR, and CuGR[a]

compound	% of CF-derived C[b]			
	GR	AgGR	AuGR	CuGR
carbon monoxide	nd	trace	nd	6
methane	3	60	19	36
chloromethane	nd	9	nd	2
dichloromethane	1	2	nd	11
chloroform	83	nd	50	nd
total C$_1$ products	87	71	69	56
ethane	trace	trace	2	trace
ethene	1	trace	2	5
acetylene	nd	1	1	nd
total C$_2$ products	2	2	4	6
total C$_3$ products	1	trace	2	3
total C$_4$ products	trace	nd	1	1
total recovered C	90	73	76	66

[a] Data are from final measurements made at 144 h (AgGR, AuGR, and CuGR) or 1152 h (GR) after the experiments were initiated by spiking with 2 μmol of CF. [b] nd indicates not detected; trace indicates detected at <1%.

Oxidation of Green Rust. The reduction of CT and CF by GR was coupled to the oxidation of Fe^{II} to Fe^{III} and resulted in the transformation of GR, AgGR, AuGR, and CuGR to a magnetic black precipitate with an XRD pattern consistent with a mixture of GR_{SO_4} and magnetite/maghemite (the XRD patterns of magnetite and the cubic form of maghemite are nearly indistinguishable) (Figure S1, Supporting Information). This observation is in agreement with the findings of Erbs et al. (29), who reported that GR_{SO_4} is oxidized by CT to magnetite.

The Fe^{II} species in our suspensions includes aqueous Fe^{II} complexes, Fe^{II} sorbed to solid phases, and structural Fe^{II} in GR and magnetite. In our experimental system, GR in equilibrium with the solution phase supports a dissolved Fe^{II} concentration of 320 μM; however, Ammonette et al. (48) observed that Fe^{2+}(aq) is unable to reduce CT, suggesting that CT reduction in GR suspensions entails heterogeneous reactions. Magnetite also contains structural Fe^{II} and has been reported to reduce CT (49); thus, it may have been a factor in the reduction of CT observed in our experiments. We did not observe degradation of CT, CF, DCM, or CM over the time scale of these experiments when we used magnetite (or magnetite with added Ag^I, Au^{III}, or Cu^{II}) as the reductant. The reactivity of magnetite with respect to the reduction of chlorinated solvents seems to exhibit considerable variability (50, 51), much of which appears to be related to differences in particle size/surface area.

Reaction Pathways and Mechanisms. The reduction of CT and CF to methane may be envisioned as resulting from a series of sequential hydrogenolysis reactions (i.e., the stepwise replacement of hydrogen for chlorine), such that CT → CF → DCM → CM → methane. However, our results suggest that the reduction of CT by GR, AgGR, AuGR, and CuGR involves processes other than sequential hydrogenolysis. A potential reaction scheme that accounts for nearly all of the products observed in our experiments is illustrated in Figure 3 (boxes indicate observed intermediates and/or products). In this reaction sequence, CT is reduced primarily to methane and other nonchlorinated end products, largely through a series of one-electron reductions forming radicals and carbenes/carbenoids.

The initial step in the reduction of halogenated hydrocarbons is commonly reported to be a single-electron transfer with the subsequent release of chloride, resulting in the formation of a radical (52−57). In the case of CT, this process results in the formation of a trichloromethyl radical (58−60) (Figure 3) that is unstable and can react by several mechanisms, including (i) accepting a second electron and abstracting a proton to form CF; (ii) coupling with a second trichloromethyl radical, forming HCA; and (iii) accepting a second electron with the subsequent release of another chloride, forming dichlorocarbene (ref 61 and references therein). The products we observed from the reduction of CT by GR (both alone and with the addition of Ag^I, Au^{III}, or Cu^{II}) are consistent with an initial one-electron reduction, resulting in the formation of a trichloromethyl radical. The levels of CF observed during CT transformation (Figure 1) suggest that hydrogenolysis is a significant pathway for the initial reduction reaction. The high levels of carbon monoxide produced during the reduction of CT by GR and CuGR (Table 1), with lesser amounts observed for AgGR and AuGR, are consistent with the formation of a dichlorocarbene (or carbenoid) intermediate; dichlorocarbene reacts readily with water to form carbon monoxide and formic acid (62). Formate was not present at detectable levels (i.e., > 2 μM) in any of our experimental systems; however, Robinson (63) showed that CO is the primary product of the reaction of dichlorocarbene with water and that formate is produced by a subsequent (and slower) reaction of carbon monoxide with hydroxide. In addition to reduction of trichloromethyl radicals, dichlorocarbene may also be produced by the hydrolysis of CF (62), which likely accounts for the carbon monoxide formed during the reduction of CF by AuGR and
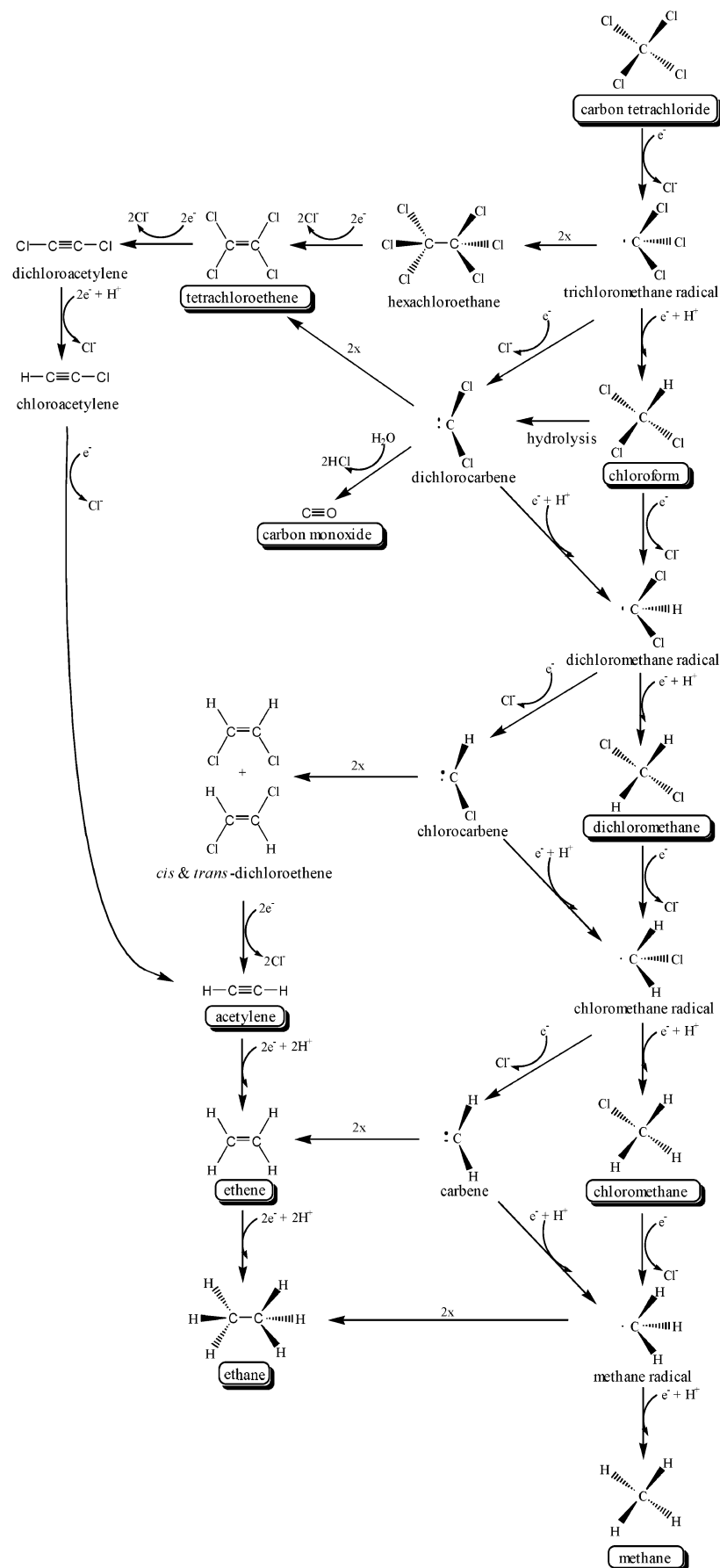
FIGURE 3. Proposed reaction scheme for the reduction of CT by GR, AgGR, AuGR, and CuGR. Boxes indicate observed intermediates/products. For simplicity, reaction pathways for the formation of C_3 and C_4 hydrocarbon products are not shown.

CuGR. Although HCA was not observed directly in any of our experiments, the production of trace levels of PCE suggests that coupling of trichloromethyl radicals to form HCA might have occurred, as HCA is rapidly reduced by GR to form PCE through a β-elimination reaction (*31*). Additionally, PCE might be formed by the coupling of dichlorocarbenes.

Although DCM and CM are products of the sequential hydrogenolysis of CT, we do not believe that they are significant intermediates in the formation of methane during the reduction of CT and CF by GR. Once formed, DCM and CM persisted throughout the course of our experiments. Furthermore, experiments independently examining the reduction of DCM and CM by GR (alone and with added Ag^{I}, Au^{III}, or Cu^{II}) showed no significant reduction of either DCM or CM over the time scale of the experiments (Table S1, Supporting Information), indicating that DCM and CM are not intermediates in the formation of methane from CT (or CF). Castro and Kray (*55*) proposed that the reduction of CT and CF by Cr^{II} in aqueous solution does not proceed via sequential hydrogenolysis but instead involves a series of single-electron transfers in which chloromethyl radicals accept an electron with the subsequent release of chloride, forming the corresponding carbene/carbenoid, which may then be reduced to a methyl radical containing one less chlorine atom (Figure 3). Such a reaction scheme does not involve DCM or CM as an intermediate; however, they may be formed by a side reaction in which dichloromethyl radicals or chloromethyl radicals accept an additional electron while abstracting a proton.

In addition to methane, a suite of C$_2$, C$_3$, and C$_4$ hydrocarbons (ethane, ethene, acetylene, propene, propane, *n*-butane, and several butene isomers) were products of the reduction of CT and CF by AgGR, AuGR, and CuGR (Tables 1 and 2); minor amounts (<1%) of ethane, ethene, and acetylene were observed as products of CT reduction by GR alone. These compounds were not observed in controls containing *n*-heptane and GR (either with or without added metals) without the addition of chlorinated methanes, indicating that the hydrocarbon products are derived from intermediates in the reduction of CT and CF. Compounds with carbon chains longer than the parent material are often identified as products of halogenated hydrocarbon reduction by reduced transition metal species (*38, 64−68*), and they are generally attributed to radical coupling reactions (*64, 66−68*). Although alkyl radicals are generally highly reactive and thus have very short lifetimes, complexation by transition metals may stabilize them, thereby increasing the probability of radical coupling reactions (*69*). As discussed earlier, the formation of PCE during CT reduction in many of our experimental systems could have resulted from the coupling of trichloromethyl radicals to form HCA, which was summarily reduced to PCE. The trace levels of ethane produced during the reduction of CT and CF by GR, AgGR, AuGR, and CuGR were not the result of reduction of ethene (as determined by independent experiments), but they may have been formed by coupling of methyl radicals (and/or carbene insertion in the C−H bond of methane).

In our proposed reaction scheme (Figure 3), acetylene may be formed through further reduction of the products of the dimerization of trichloromethyl radicals, dichlorocarbene, and/or chlorocarbene. The reduction of PCE by β-elimination produces dichloroacetylene (DCAc), which can be further reduced to chloroacetylene (CAc) and then acetylene (*70, 71*). We did not observe DCAc or CAc as intermediates in the reduction of CT; however, DCAc and CAc are likely to be highly reactive intermediates in our experimental system, and thus they would not be expected to accumulate to levels detectable by our analytical methods. Lee and Batchelor (*30*) reported that acetylene is the main transformation product of the reduction of PCE by GR. Although these authors did not observe DCAc and CAc as intermediates in the reduction of PCE to acetylene, their data are consistent with the reaction sequence PCE → DCAc → CAc → acetylene.

The coupling of carbenes is typically considered to be unlikely, largely because of their highly reactive nature and the correspondingly low probability of two carbene molecules interacting as well as rapid dimer dissociation resulting from high excess internal energy (*72, 73*). Although these limitations are consistent with conditions in homogeneous systems (particularly in vapor-phase reactions), in heterogeneous systems (like the ones examined in this study) the proposed carbene intermediates likely exist as surface complexes (carbenoids), which may increase their relative stability. The presence of solvent molecules also offers a means of dissipating the excess internal energy of potential coupling products, lowering the likelihood of dissociation. Potentially longer lifetimes and localization on surfaces would increase the likelihood of carbene-coupling reactions. Indeed, several studies have suggested that carbene coupling does occur in systems that promote the stability and/or physical proximity of carbenes/carbenoids (*74−77*). Independent experiments examining the reduction of acetylene by GR, AgGR, AuGR, and CuGR indicated that the kinetics of acetylene reduction to ethene are too slow to account for the accumulation of ethene in our CT and CF reduction experiments, suggesting that parallel reactions (e.g., carbene coupling) are involved.

The C$_3$ and C$_4$ hydrocarbons (propane, propene, *n*-butane, and butene isomers) produced during the reduction of CT (and, to a lesser extent, CF) by AgGR, AuGR, and CuGR may have resulted from coupling reactions of radicals and/or carbenes as well as insertion of carbene into C−H bonds of smaller-chain hydrocarbons (e.g., ethane + carbene → propane) (*73*).

Mechanism(s) of the Catalytic Effects of Ag, Au, and Cu. Although the reductive transformation of many contaminants (including many halogenated hydrocarbons) is thermodynamically favorable under suboxic conditions, these reactions are often kinetically limited. However, in the presence of a suitable bulk reductant, many transition metal complexes have been shown to be effective catalysts for redox reactions (*35, 38, 53, 56, 57*). Typically, the catalytic effect has been attributed to facilitated transfer of electrons from a bulk reductant to the oxidant of interest through a cycling of the metal between reduced and oxidized forms. Copper(II) has been shown to catalyze the oxidation by molecular oxygen of structural Fe^{II} in vermiculatized biotite (*78*); the proposed mechanism involves facilitated electron transfer via Cu^{II}/Cu^{I} cycling. The reduction of nitrate by Fe^{II} is catalyzed by the addition of Cu^{II}, Ag^{I}, and Hg^{II} (*39, 79*). Although no specific mechanism has been proposed, Ottley et al. (*39*), suggested that the catalytic effect is due to solid-phase Cu, Ag, or Hg, either sorbed to iron oxide surfaces or as a bulk mineral phase.

Recently, examination of AgGR, AuGR, and CuGR and by X-ray absorption fine structure (XAFS) spectroscopy and high-resolution transmission electron microscopy has revealed that Ag^{I}, Au^{III}, and Cu^{II} are reduced by GR to Ag^{0}, Au^{0}, and Cu^{0}, which are present as submicron-sized particles (*80*). The enhanced reduction of CT by AgGR, AuGR, and CuGR may be analogous to the enhanced reduction of chlorinated hydrocarbons by bimetallic reductants (*34, 42, 43, 81−83*), which are composed of a noble metal (typically, Pd, Pt, or Ni) plated onto a more active metal (e.g., Fe, Zn). Although the exact mechanism(s) by which the catalysis occurs in most bimetallic systems are not fully understood, coupling of a less reactive (noble) metal to a more reactive metal to accelerate the oxidation of the more reactive metal is well-known (*84*). The coupled active and noble metals form galvanic cells where the active metal serves as the anode and is oxidized, while reduction of the chlorinated hydrocarbon

(or other oxidant) occurs at the noble metal (cathode). As surface-associated particles, reduced metals coupled to GR may similarly form galvanic cells in which the GR serves as the anode and is oxidized, while CT is reduced at the metal surface.

The reduction of CT by nanoparticulate Ag^0, Au^0, and Cu^0 was examined to determine whether CT is degraded by these metals in the absence of GR. There was no measurable change in the CT concentrations in the vials containing Ag^0 or Au^0. This was expected because the coupling of Ag^0 or Au^0 oxidation to the reduction of CT is not thermodynamically favorable. However, it is thermodynamically feasible to reduce CT with Cu^0, and 10 μmol CT was reduced below detectable levels within 26 h by nanoparticulate Cu^0. However, the only identified products of CT reduction by Cu^0 were CO (18%) and formate (27%); CF, DCM, CM, and nonchlorinated hydrocarbons (which are products of CT reduction by CuGR) were not observed, suggesting that direct reduction of CT by Cu^0 is not a significant reaction during the reduction of CT by CuGR.

Differences in the reduction rates of CT among AgGR, AuGR, and CuGR as well as variations in product distributions (e.g., the greater abundance of coupling products observed for CT reduction by AuGR, see Table 1) are likely due to differences in the surface atomic structure and electronic properties of Ag^0, Au^0, and Cu^0. Similar observations have been reported for related systems. Liu et al. have reported that the kinetics and product distribution of the electrolytic reduction of CT depend on the type of metal used for the cathode (85). Differences in reductions rates are also observed within series of bimetallic reductants (e.g., PdFe, PtFe, NiFe). The rates of trichloroethene (TCE) reduction by PdFe and PdZn are greater than those for NiFe or NiZn, respectively (43); similarly, TCE reduction by PdFe is faster than by PtFe (34). It has been suggested that the enhanced reduction observed with PdFe (relative to Fe^0 alone) is largely due to the accumulation of H_2 generated from the reduction of water by Fe^0 at the Pd^0–water interface (86). Indeed, Pd^0 has been shown to be an effective catalyst for the reduction of chlorinated solvents by H_2 (87). However, in our experiments the rate of CT reduction in replicate experiments was independent of H_2 concentration in the headspace, and thus it is unlikely that a similar catalytic process is occurring with AgGR, AuGR, and CuGR.

Environmental Significance. Zerovalent iron has been the most extensively studied reductant for the treatment of groundwater contaminated with chlorinated hydrocarbons and is currently the most commonly used material for the construction of PRBs (33). However, a thorough understanding of the processes involved in the reduction of chlorinated hydrocarbons by Fe^0 is lacking. In particular, little is known regarding the role of Fe^{II} species in the reduction of chlorinated hydrocarbons in Fe^0 systems (88). Green rusts have been observed as products in Fe^0 columns and PRBs (89–91), and Williams and Scherer (28) suggested that the formation of Fe^{II}-bearing minerals such as GRs contributes to the long-term effectiveness of Fe^0 PRBs despite the formation of thick oxide films. Moreover, our results showing the catalytic effects of AgGR, AuGR, and CuGR on the reduction of CT and CF may enhance our collective understanding of the dechlorination pathways for chlorinated organic contaminants by bimetallic and other catalytic systems.

Our results along with other studies of the reduction of CT, halogenated ethanes, and chlorinated ethenes by GR (29–31) suggest that GR may be useful for the remediation of chlorinated hydrocarbon contamination in the subsurface. Green rusts can be easily prepared from relatively inexpensive commodity chemicals (e.g., ferrous sulfate (copperas) and sodium hydroxide (caustic soda)). Injection and dispersion of synthetic GR suspensions into the subsurface may provide an alternative to standard Fe^0 PRBs. In addition, the enhanced reduction of CT and CF by AgGR, AuGR, and CuGR may prove useful in the development of improved materials for PRBs and other remediation technologies.

Supporting Information Available

One figures and one table. This material is available free of charge via the Internet at http://pubs.acs.org.

Literature Cited

(1) Bigham, J. M.; Tuovinen, O. H. In *Planetary Ecology*; Caldwell, D. E., Brierley, J. A., Brierley, C. L., Eds.; Van Nostrand Reinhold Co.: New York, 1985; pp 239–250.

(2) Génin, J.-M. R.; Refait, P.; Olowe, A. A.; Abdelmoula, M.; Fall, I.; Drissi, S. H. *Hyperfine Interact.* **1998**, *112*, 47–50.

(3) Kumar, A. V. R.; Singh, R.; Nigam, R. K. *J. Radioanal. Nucl. Chem.* **1999**, *242*, 131–137.

(4) Refait, P.; Abdelmoula, M.; Génin, J.-M. R. *Corros. Sci.* **1998**, *40*, 1547–1560.

(5) Ona-Nguema, G.; Abdelmoula, M.; Jorand, F.; Benali, O.; Géhin, A.; Block, J.-C.; Génin, J.-M. R. *Environ. Sci. Technol.* **2002**, *36*, 16–20.

(6) Fredrickson, J. K.; Zachara, J. M.; Kennedy, D. W.; Dong, H.; Onstott, T. C.; Hinman, N. W.; Li, S.-M. *Geochim. Cosmochim. Acta* **1998**, *62*, 3239–3257.

(7) Tamaura, Y.; Saturno, M.; Yamada, K.; Katsura, T. *Bull. Chem. Soc. Jpn.* **1984**, *57*, 2417–2421.

(8) Taylor, R. M. *Clay Miner.* **1980**, *15*, 369–382.

(9) Chaudhuri, S. K.; Lack, J. G.; Coates, J. D. *Appl. Environ. Microbiol.* **2001**, *67*, 2844–2848.

(10) Refait, P.; Drissi, S. H.; Pytkiewicz, J.; Génin, J.-M. R. *Corros. Sci.* **1997**, *39*, 1699–1710.

(11) Schwertmann, U.; Fechter, H. *Clay Miner.* **1994**, *29*, 87–92.

(12) Olowe, A. A.; Marie, Y.; Refait, P.; Génin, J.-M. R. *Hyperfine Interact.* **1994**, *93*, 1783–1788.

(13) Perez, O. P.; Umetsu, Y.; Sasaki, H. *Hydrometallurgy* **1998**, *50*, 223–242.

(14) Refait, P.; Génin, J.-M. R. *Corros. Sci.* **1997**, *39*, 539–553.

(15) Schwertmann, U.; Taylor, R. M. In *Minerals in Soil Environments*; Dixon, J. B., Weed, S. B., Eds.; Soil Science Society of America: Madison, WI, 1977; pp 145–180.

(16) Srinivasan, R.; Lin, R.; Spicer, R. L.; Davis, B. H. *Colloids Surf. A* **1996**, *113*, 97–105.

(17) Lin, R.; Spicer, R. L.; Tungate, F. L.; Davis, B. H. *Colloids Surf. A* **1996**, *113*, 79–96.

(18) Ponnamperuma, F. N.; Tianco, E. M.; Loy, T. *Soil Sci.* **1967**, *103*, 374–382.

(19) Abdelmoula, M.; Trolard, F.; Bourrié, G.; Génin, J.-M. R. *Hyperfine Interact.* **1998**, *112*, 235–238.

(20) Trolard, F.; Génin, J.-M. R.; Abdelmoula, M.; Bourrié, G.; Humbert, B.; Herbillon, A. *Geochim. Cosmochim. Acta* **1997**, *61*, 1107–1111.

(21) Génin, J.-M. R.; Bourrié, G.; Trolard, F.; Abdelmoula, M.; Jaffrezic, A.; Refait, P.; Maitre, V.; Humbert, B.; Herbillon, A. *Environ. Sci. Technol.* **1998**, *32*, 1058–1068.

(22) Bourrié, G.; Trolard, F.; Génin, J.-M. R.; Jaffrezic, A.; Maître, V.; Abdelmoula, M. *Geochim. Cosmochim. Acta* **1999**, *63*, 3417−3427.

(23) O'Loughlin, E. J.; Kelly, S. D.; Csencsits, R.; Cook, R. E.; Kemner, K. M. *Environ. Sci. Technol.* **2003**, *37*, 721−727.

(24) Hansen, H. C. B.; Borggaard, O. K.; Sorensen, J. *Geochim. Cosmochim. Acta* **1994**, *58*, 2599−2608.

(25) Koch, C. B.; Hansen, H. C. B. *Adv. GeoEcol.* **1997**, *30*, 373−393.

(26) Myneni, S. C. B.; Tokunaga, T. K.; Brown, G. E., Jr. *Science* **1997**, *278*, 1106−1109.

(27) Loyaux-Lawniczak, S.; Refait, P.; Lecomte, P.; Ehrhardt, J.-J.; Génin, J.-M. R. *Hydrol. Earth Syst. Sci.* **1999**, *3*, 593−599.

(28) Williams, A. G. B.; Scherer, M. M. *Environ. Sci. Technol.* **2001**, *35*, 3488−3494.

(29) Erbs, M.; Hansen, H. C. B.; Olsen, C. E. *Environ. Sci. Technol.* **1999**, *33*, 307−311.

(30) Lee, W.; Batchelor, B. *Environ. Sci. Technol.* **2002**, *36*, 5348−5354.

(31) O'Loughlin, E. J.; Burris, D. R. *Environ. Toxicol. Chem.* (in press).

(32) Scherer, M. M.; Balko, B. A.; Gallagher, D. A.; Tratnyek, P. G. *Environ. Sci. Technol.* **1998**, *32*, 3026−3033.

(33) Scherer, M. M.; Richter, S.; Valentine, R. L.; Alvarez, P. J. J. *Crit. Rev. Environ. Sci. Technol.* **2000**, *30*, 363−411.

(34) Cheng, S.-F.; Wu, S.-C. *Chemosphere* **2000**, *41*, 1263−1270.

(35) Gantzer, C. J.; Wackett, L. P. *Environ. Sci. Technol.* **1991**, *25*, 715−722.

(36) Ma, H.; O'Loughlin, E. J.; Burris, D. R. *Environ. Sci. Technol.* **2001**, *35*, 717−724.

(37) Nelson, D. W.; Bremner, J. M. *Soil Biol. Biochem.* **1970**, *2*, 1−8.

(38) O'Loughlin, E. J.; Burris, D. R.; Delcomyn, C. A. *Environ. Sci. Technol.* **1999**, *33*, 1145−1147.

(39) Ottley, C. J.; Davison, W.; Edmunds, W. M. *Geochim. Cosmochim. Acta* **1997**, *61*, 1819−1828.

(40) Pettine, M.; Barra, I.; Campanella, L.; Millero, F. *Water Res.* **1998**, *32*, 2807−2813.

(41) Schwarzenbach, R. P.; Stierli, R.; Lanz, K.; Zeyer, J. *Environ. Sci. Technol.* **1990**, *24*, 1566−1574.

(42) Xu, Y.; Zhang, W.-x. *Ind. Eng. Chem. Res.* **2000**, *39*, 2238−2244.

(43) Zhang, W.-x.; Wang, C.-B.; Lien, H.-L. *Catal. Today* **1998**, *40*, 387−395.

(44) Cornell, R. M.; Schwertmann, U. *The Iron Oxides: Structure, Properties, Reactions, Occurrence and Uses*; VCH Publishers: New York, 1996.

(45) Hansen, H. C. B.; Koch, C. B. *Clay Miner.* **1998**, *33*, 87−101.

(46) Burris, D. R.; Delcolymn, C. A.; Smith, M. H.; Roberts, A. L. *Environ. Sci. Technol.* **1996**, *30*, 3047−3052.

(47) Gossett, J. M. *Environ. Sci. Technol.* **1987**, *21*, 202−208.

(48) Amonette, J. E.; Workman, D. J.; Kennedy, D. W.; Fruchter, J. S.; Gorby, Y. A. *Environ. Sci. Technol.* **2000**, *34*, 4606−4613.

(49) McCormick, M. L.; Bouwer, E. J.; Adriaens, P. *Environ. Sci. Technol.* **2002**, *36*, 403−410.

(50) Curtis, G. P. Ph.D. Dissertation, Stanford University, Palo Alto, CA, 1991.

(51) McCormick, M. L.; Kim, H. S.; Bouwer, E. J.; Adriaens, P. Abiotic transformation of chlorinated solvents as a consequence of microbial iron reduction: An investigation of the role of biogenic magnetite in mediating reductive dechlorination. *Thirtieth Mid-Atlantic Industrial and Hazardous Waste Conference− Hazardous and Industrial Wastes*; 1998; pp 339−348.

(52) Andrieux, C. P.; Gallardo, I.; Savéant, J.-M.; Su, K.-B. *J. Am. Chem. Soc.* **1986**, *108*, 638−647.

(53) Bakac, A.; Espenson, J. H. *J. Am. Chem. Soc.* **1986**, *108*, 713−719.

(54) Buschmann, J.; Angst, W.; Schwarzenbach, R. P. *Environ. Sci. Technol.* **1999**, *33*, 1015−1020.

(55) Castro, C. E.; Kray, W. C., Jr. *J. Am. Chem. Soc.* **1966**, *88*, 4447−4455.

(56) Glod, G.; Angst, W.; Holliger, C.; Schwarzenbach, R. *Environ. Sci. Technol.* **1997**, *31*, 253−260.

(57) Wade, R. S.; Castro, C. E. *J. Am. Chem. Soc.* **1973**, *95*, 226−230.

(58) Assaf-Anid, N.; Hayes, K. F.; Vogel, T. M. *Environ. Sci. Technol.* **1994**, *28*, 246−252.

(59) Lewis, T. A.; Paszczynski, A.; Gordon-Wylie, S. W.; Jeedigunta, S.; Lee, C.-H.; Crawford, R. L. *Environ. Sci. Technol.* **2001**, *35*, 552−559.

(60) Poyer, J. L.; Floyd, R. A.; McCay, P. B.; Janzen, E. G.; Davis, E. R. *Biochim. Biophys. Acta* **1978**, *539*, 402−409.

(61) Criddle, C. S.; McCarty, P. L. *Environ. Sci. Technol.* **1991**, *25*, 973−978.

(62) Hine, J. *J. Am. Chem. Soc.* **1950**, *72*, 2438−2445.

(63) Robinson, E. A. *J. Chem. Soc.* **1961**, 1663−1671.

(64) Bakac, A.; Espenson, J. H. *J. Am. Chem. Soc.* **1986**, *108*, 719−723.

(65) Campbell, T. J.; Burris, D. R.; Roberts, A. L.; Wells, J. R. *Environ. Toxicol. Chem.* **1997**, *16*, 625−630.

(66) Castro, C. E.; Kray, W. C., Jr. *J. Am. Chem. Soc.* **1963**, *85*, 2768−2773.

(67) Fennelly, J. P.; Roberts, A. L. *Environ. Sci. Technol.* **1998**, *32*, 1980−1988.

(68) Helvenston, M. C.; Castro, C. E. *J. Am. Chem. Soc.* **1992**, *114*, 8490−8496.

(69) Kochi, J. K.; Rust, F. F. *J. Am. Chem. Soc.* **1961**, *83*, 2017−2018.

(70) Arnold, W. A.; Roberts, A. L. *Environ. Sci. Technol.* **1998**, *32*, 3017−3025.

(71) Roberts, A. L.; Totten, L. A.; Arnold, W. A.; Burris, D. R.; Campbell, T. J. *Environ. Sci. Technol.* **1996**, *30*, 2654−2659.

(72) Harris, J. M.; Wamser, C. C. *Fundamentals of Organic Reaction Mechanisms*; John Wiley & Sons: New York, 1976.

(73) March, J. *Advanced Organic Chemistry: Reactions, Mechanisms, and Structure,* 4th ed.; John Wiley & Sons: New York, 1992.

(74) Baratta, W.; Del Zotto, A.; Rigo, P. *Organometallics* **1999**, *18*, 5091−5096.

(75) Beckhaus, R. *J. Chem. Soc., Dalton Trans.* **1997**, 1991−2001.

(76) Borer, M.; Loosli, T.; Minger, A.; Neuenschwander, M.; Engel, P. *Helv. Chim. Acta* **1995**, *78*, 1311−1324.

(77) Dötz, K. H.; Siemoneit, S.; Hohmann, F.; Nieger, M. *J. Organomet. Chem.* **1997**, *541*, 285−290.

(78) Sayin, M. *Clays Clay Miner.* **1982**, *30*, 287−290.

(79) Buresh, R. J.; Moraghan, J. T. *J. Environ. Qual.* **1976**, *5*, 320−325.

(80) O'Loughlin, E. J.; Kelly, S. D.; Kemner, K. M.; Csencsits, R.; Cook, R. E. *Chemosphere* (in press).

(81) Lien, H.-L.; Zhang, W.-x. *J. Environ. Eng.* **1999**, *125*, 1042−1047.

(82) Muftikian, R.; Fernando, Q.; Korte, N. *Water Res.* **1995**, *29*, 2434−2439.

(83) Wan, C.; Chen, Y. H.; Wei, R. *Environ. Toxicol. Chem.* **1999**, *18*, 1091−1096.

(84) Jones, D. A. *Principles and Prevention of Corrosion*; Prentice-Hall: Englewood Cliffs, NJ, 1992.

(85) Liu, Z.; Arnold, R. G.; Betterton, E. A.; Festa, K. D. *Environ. Eng. Sci.* **1999**, *16*, 1−13.

(86) Grittini, C.; Malcomson, M.; Fernando, Q.; Korte, N. *Environ. Sci. Technol.* **1995**, *29*, 2898−2900.

(87) Lowry, G. V.; Reinhard, M. *Environ. Sci. Technol.* **1999**, *33*, 1905−1910.

(88) Scherer, M. M.; Balko, B. A.; Tratnyek, P. G. In *Kinetics and Mechanisms of Reactions at the Mineral-Water Interface*; Sparks, D. L., Grundl, T. J., Eds.; American Chemical Society: Washington, DC, 1998; pp 301−332.

(89) Furukawa, Y.; Kim, J.-W.; Watkins, J.; Wilkin, R. T. *Environ. Sci. Technol.* **2002**, *36*, 5469−5475.

(90) Gu, B.; Phelps, T. J.; Liang, L.; Dickey, M. J.; Roh, Y.; Kinsall, B. L.; Palumbo, A. V.; Jacobs, G. K. *Environ. Sci. Technol.* **1999**, *33*, 2170−2177.

(91) Roh, Y.; Lee, S. Y.; Elless, M. P. *Environ. Geol.* **2000**, *40*, 184−194.

Environmental Science and Technology: Supporting Information

Effects of Ag^I, Au^{III}, and Cu^{II} on the Reductive Dechlorination of Carbon Tetrachloride by Green Rust

Edward J. O'Loughlin, Kenneth M. Kemner, and David R. Burris
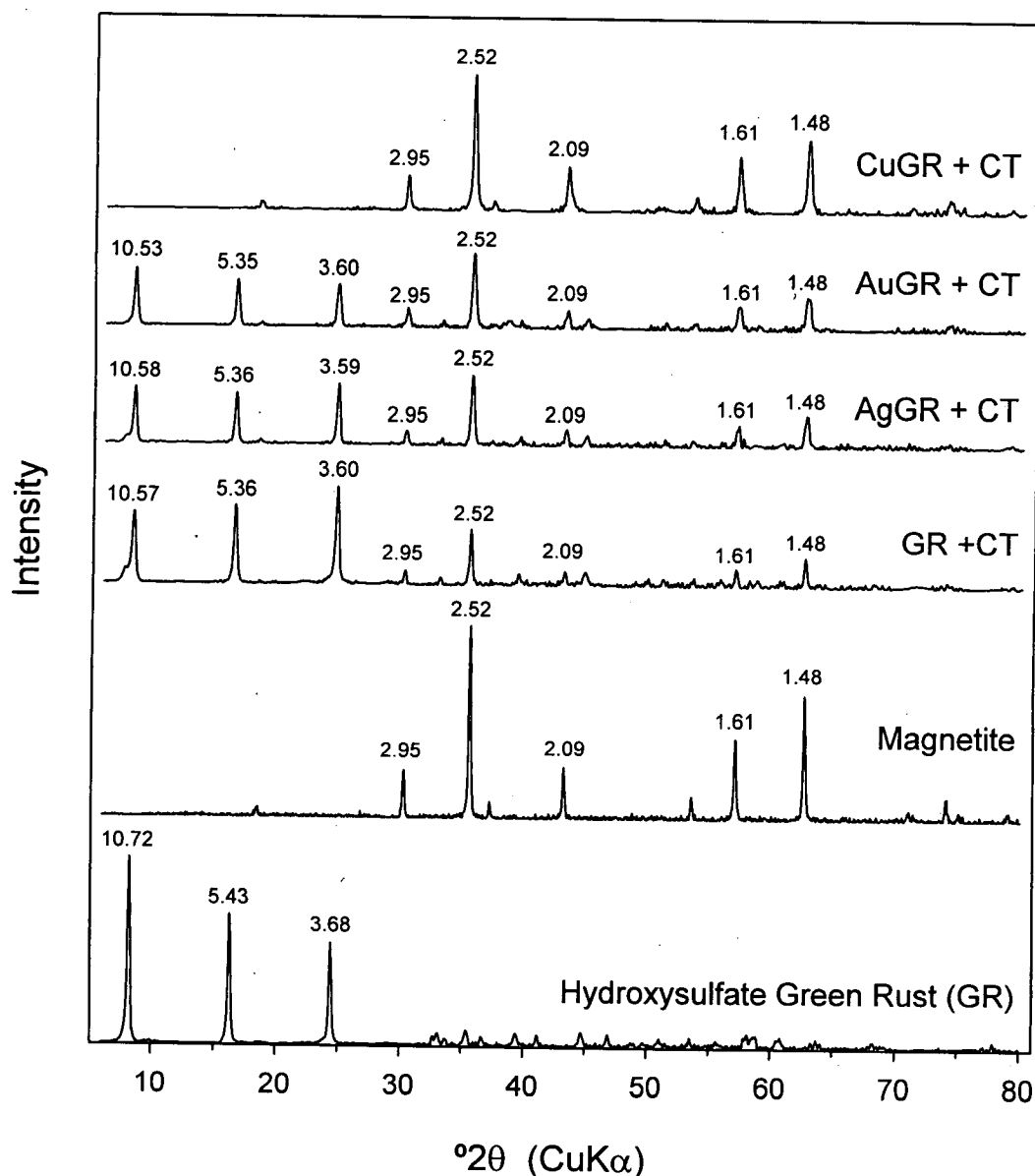
Figure S1. Comparison of XRD patterns of GR$_{SO_4}$ and magnetite with the patterns of GR$_{SO_4}$, AgGR, AuGR, and CuGR 5 days after the addition of 10 μmol CT. Scans were made between 6° and 80° at a rate of 1° min^{-1}. The values located above the major peaks indicate the corresponding *d*-spacings (Å).

Table S1. Final product distributions for DCM and CM reduction by GR, AgGR, AuGR, and CuGR[a]

Compound	% of DCM- or CM-derived C[b]			
	GR	AgGR	AuGR	CuGR
Dichloromethane				
Methane	nd	3	nd	3
Chloromethane	nd	5	nd	nd
Dichloromethane	98	88	97	97
Total recovered C	98	96	97	100
Chloromethane				
Methane	nd	trace	nd	trace
Chloromethane	92	91	96	94
Total recovered C	92	91	96	94

[a]Data are from final measurements made at 144 h (AuGR) or 1,152 h (GR, AgGR, and CuGR), after the experiments were initiated by spiking with 2 μmol of DCM or CM. [b]"nd" indicates not detected; "trace" indicates detected at < 1%.